THE ASTROPHYSICAL JOURNAL 243:841–854, 1981 February 1

THE OLD OPEN CLUSTER NGC 2506 AND ITS SIMILARITY TO NGC 2420

ROBERT D. MCCLURE[1]
Dominion Astrophysical Observatory, Herzberg Institute of Astrophysics and
Yale University Observatory
BRUCE A. TWAROG
Yale University Observatory
AND
WILLIAM T. FORRESTER[1]
University of Southern California and Yale University Observatory
Received 1979 December 10; accepted 1980 August 13

ABSTRACT

Photoelectric photometry on the *UBV* and DDO systems and photographic photometry in *B* and *V* are presented for stars in the open cluster NGC 2506. The derived ultraviolet excess $\delta(U-B) = 0.09$ mag, and CN anomaly $\delta CN = -0.08$ mag imply a low heavy-element abundance ([Fe/H] = −0.55) relative to the Hyades. The photographic photometry is combined with proper motion data of Chiu and van Altena to construct a color-magnitude diagram for the cluster members. The derived age of 3.4×10^9 years is similar to that of M67 from fits to the same grid of isochrones. The distance modulus of 12.2 mag corresponds to a position for NGC 2506 of almost 3 kpc near the direction of the galactic anticenter, and 500 pc above the plane.

The characteristic of low metallicity for an old disk cluster, together with its galactocentric position several kpc beyond the solar orbit place this cluster into a class of similar objects that includes NGC 2420 as the prototype, NGC 2158, NGC 2204, NGC 2243, and Melotte 66.

It is estimated that approximately half of the stars on the main sequence of NGC 2506 are binaries.

Subject headings: clusters: open — stars: abundances

I. INTRODUCTION

Until recently, much of our knowledge about the stellar population of the old disk component of the Galaxy was derived primarily from observations of only two well-studied old clusters, M67 and NGC 188. Both of these clusters have near-solar metal abundance and are located at galactocentric distances near the solar distance. The work of McClure, Forrester, and Gibson (1974) on NGC 2420 provided the first example of a well-studied disk cluster that is significantly metal-poor relative to the Sun. At the time of their study NGC 2420 was an isolated exception to the metal-rich disk population of clusters, although Arp (1962) had suggested that several clusters in the anticenter region of the Galaxy have ultraviolet excesses.

With the completion of work on NGC 2420, a series of observations was begun on the open cluster NGC 2506 ($\alpha_{1900} = 7^h\ 55^m.2$, $\delta_{1900} = -10°\ 31'$). This cluster was included in King's (1964) list of clusters with ages probably greater than the Hyades, a prediction corroborated by the later preliminary photographic work on the cluster by Purgathofer (1964). Its position at relatively high galactic latitude near the direction of the galactic anticenter ($l = 230°.6$; $b = +9°.9$) made it a likely candidate to be an NGC 2420 type of object. In addition, the existence of a deep first-epoch plate offered the possibility of separating field stars from cluster members, a feature which made NGC 2420 data so valuable. The accompanying proper motion study of NGC 2506 by Chiu and van Altena (1981) now makes a detailed discussion of this interesting cluster feasible.

II. OBSERVATIONS

a) *UBV Photometry*

A photoelectric sequence of 38 stars was observed in NGC 2506 using the Yale–CTIO 1 m telescope on Cerro Tololo during the period 1975 January to 1977 January. These observations were taken on several runs with various pulse-counting systems including single channel 1P21 photometers and two-channel S-20 photometers with standard Cerro Tololo filter sets appropriately blocked for the system. Cousins (1973) E region and Landolt's (1973) equatorial standards were used to transform the data to the *UBV* system. The adopted magnitudes and colors are listed in Table 1. The column labeled "*n*" indicates the number of nights on which each star was observed.

Photographic plates were also obtained for the cluster with the 1 m and 1.5 m telescopes during several of the same observing runs. We have measured six *V* and seven *B* plates. Table 2 lists the characteristics of this plate material.

[1] Visiting Astronomer, Cerro Tololo Inter-American Observatory, supported by the National Science Foundation under contract No. AST 78-27879.

TABLE 1

PHOTOELECTRIC UBV PHOTOMETRY

Star	P (%)	V	$B-V$	$U-B$	n	$\delta(U-B)$
(1)	(2)	(3)	(4)	(5)	(6)	(7)
1112	65	12.95	0.98	0.60	2	0.15
1136	95	14.70	0.40	−0.01	1	0.17
2111	0	11.59	0.57	0.11	2	
2122	92	11.73	1.13	0.98	2	0.07
4101	94	15.92	0.42	...	1	
4125	92	15.63	0.36	...	2[a]	
4128	...	13.02	0.88	0.50	2	
4150	83	16.71	0.59	...	3	
1253	93	17.77	0.76	...	2	
1254	92	16.89	0.54	...	2	
1258	95	15.65	0.41	−0.04	1	0.15
2212	95	11.95	1.07	0.83	2	0.10
2283	94	15.21	0.38	0.07	2[a]	0.05
3204	93	12.66	0.90	0.54	3	0.05
3206	94	14.88	0.43	0.01	2[a]	0.12
3213	81	14.33	0.59	0.09	2[a]	0.07
3231	91	13.12	0.98	0.60	2	0.15
3239	94	14.98	0.43	0.06	1	0.06
3241	94	13.84	0.10	0.09	2	
3248	1	17.18	0.52	...	2	
3254	20	11.13	1.41	1.48	2	
3255	71	13.06	0.86	0.48	1	0.03
3258	61	16.36	0.52	...	1	
3265	91	13.19	1.04	0.58	1	0.29
3270	70	16.62	0.52	...	1	
4228	0	12.00	1.66	1.72	2	
4240	79	13.13	0.99	0.69	2	0.08
4241	93	15.09	0.41	0.06	1	0.06
4254	62	14.96	0.45	0.11	1	0.00
4277	...	17.97	0.68	...	2	
1305	94	14.31	0.38	...	1	
3392	14	13.12	0.91	0.50	1	
4331	...	15.18	0.39	...	2	
2401	...	11.09	1.59	1.94	3	
2402	...	12.45	1.19	1.07	3	
3401	...	11.64	0.93	0.66	2	
4401	...	11.86	0.64	0.17	3	
4402	...	12.58	1.73	2.08	2	

[a] One $U-B$ observation only.

TABLE 2

DATA ON PHOTOGRAPHIC EXPOSURES

Telescope	Plate	Date	Emulsion	Filter	Exposure (min.)
1 m	1192	1975 Dec 11/12	103aO	GG385	60
	1193	1975 Dec 11/12	103aO	GG385	45
	1194	1975 Dec 11/12	103aO	GG385	50
	1197	1975 Dec 11/12	103aD	GG495	80
	1389	1976 Jan 10/11	103aD	GG495	15
	1390	1976 Jan 10/11	103aO	GG385	50
	1391	1976 Jan 11/12	103aD	GG495	70
	1392	1976 Jan 11/12	103aO	GG385	30
	1395	1976 Jan 12/13	103aD	GG495	30
	1397	1976 Jan 12/13	103aO	GG385	15
	1398	1976 Jan 12/13	103aO	GG385	50
1.5 m	2706	1975 Dec 12/13	103aD	GG495	45
	2707	1975 Dec 12/13	103aD	GG495	45

TABLE 3 PHOTOGRAPHIC VALUES

STAR	V	B-V	STAR	V	B-V	STAR	V	B-V	STAR	V	B-V
1101	15.59	0.38	2103	17.87	0.69	2145	17.23	0.59	3132	15.40	0.37
1102	17.79	0.59	2104	17.28	0.66	2146	16.24	0.59	3133	15.96	0.39
1103	16.88	0.53	2105	17.43	1.09	2147	16.25	0.44	3134	15.05	0.79
1104	17.45	0.67	2107	15.69	0.56	2148	15.74	0.37	3135	14.97	0.39
1105	16.60	0.50	2108	15.35	0.43	2149	15.57	0.38	3136	14.93	0.37
1106	14.81	0.39	2109	13.15	0.94	2150	16.81	0.73	3137	15.27	0.33
1107	16.32	0.52	2110	13.74	0.45	2152	15.60	0.36	3138	16.68	0.45
1108	14.60	0.77	2111	11.47	0.57	3101	16.86	0.53	3139	17.18	0.65
1111	15.54	0.42	2112	14.31	0.38	3103	15.18	0.36	3140	17.57	0.57
1112	12.95	1.00	2113	14.88	0.39	3104	15.49	0.38	3141	16.57	0.50
1113	14.55	0.42	2114	15.98	0.42	3105	15.04	0.40	3142	16.92	0.46
1114	15.70	0.96	2117	15.55	0.39	3106	17.67	0.64	3143	14.97	0.26
1115	16.06	0.44	2118	14.54	0.37	3107	15.10	0.40	3144	16.92	0.59
1116	15.44	0.43	2120	15.56	0.41	3108	15.47	0.36	3145	15.84	0.36
1117	17.40	0.63	2121	15.68	0.37	3109	15.80	0.56	3147	10.76	0.37
1118	17.49	0.79	2122	11.69	1.16	3110	14.71	0.88	3148	15.57	0.47
1119	16.26	0.49	2124	15.47	0.42	3111	14.50	0.44	3149	16.99	0.62
1120	15.41	0.38	2125	16.17	0.58	3112	14.62	0.36	3150	16.15	0.43
1121	16.39	0.46	2126	17.70	0.76	3113	17.83	0.63	3151	16.01	0.48
1122	15.22	0.36	2127	15.90	0.42	3114	17.94	0.74	3152	14.91	0.41
1123	16.77	0.59	2128	16.71	0.65	3115	17.32	0.58	3153	17.27	0.55
1124	15.39	0.37	2129	14.78	0.46	3116	13.93	0.78	3154	16.07	0.50
1125	14.95	0.39	2130	17.00	0.60	3118	15.55	0.32	3155	15.50	0.23
1126	16.28	0.47	2131	17.83	0.66	3119	15.00	0.43	3156	15.42	0.28
1127	15.06	0.40	2132	15.55	0.36	3120	16.36	0.52	3157	15.16	0.36
1128	17.77	0.68	2133	16.36	0.47	3121	15.58	0.46	3158	14.72	0.40
1129	14.82	0.62	2134	15.13	0.33	3122	17.66	0.64	3159	16.92	0.53
1130	16.93	0.68	2135	17.34	0.64	3123	17.65	0.69	3161	14.41	0.46
1131	17.21	0.61	2136	15.98	0.49	3124	17.70	0.54	3162	16.55	0.43
1134	15.06	0.41	2137	16.16	0.54	3125	17.64	0.65	3163	17.48	0.65
1135	15.11	0.32	2138	17.91	0.67	3126	17.59	0.62	3164	16.93	0.53
1136	14.65	0.51	2139	14.75	0.41	3128	15.06	0.36	4101	15.90	0.38
1137	17.32	0.66	2140	14.02	0.41	3129	14.72	0.31	4102	15.84	0.43
2101	11.96	0.89	2143	17.01	0.67	3130	17.19	0.68	4103	16.86	0.70
2102	14.91	0.43	2144	14.40	0.45	3131	16.42	0.45	4104	15.57	0.37

TABLE 3—*Continued*

STAR	V	B-V	STAR	V	B-V	STAR	V	B-V	STAR	V	B-V
4105	15.34	0.33	4148	17.74	0.74	1231	16.03	0.55	1270	17.91	0.69
4106	14.21	0.37	4149	15.48	0.39	1232	17.56	0.92	1271	16.32	0.61
4108	16.61	0.56	4150	16.67	0.58	1233	15.31	0.96	1272	17.39	0.66
4109	13.77	0.85	4151	17.27	0.67	1234	17.38	0.65	2201	17.71	0.81
4110	16.29	0.57	4152	14.34	0.39	1235	15.37	0.36	2202	17.64	0.81
4111	17.80	0.60	4153	17.44	0.67	1236	17.73	0.66	2203	17.96	0.69
4112	16.16	0.54	4154	16.20	0.50	1237	16.20	0.45	2204	17.72	0.70
4113	15.79	1.36	1201	15.98	1.07	1238	17.84	0.62	2205	16.74	0.52
4114	14.95	0.40	1202	17.13	0.63	1239	17.74	0.69	2206	15.67	0.41
4117	13.66	0.26	1203	14.23	0.27	1240	15.70	0.47	2207	18.06	0.67
4118	14.98	0.32	1204	16.32	0.47	1241	14.84	0.41	2209	14.84	0.58
4119	15.89	0.37	1205	15.65	0.40	1242	16.66	0.49	2210	15.45	0.41
4121	16.13	0.53	1206	15.43	1.16	1243	17.61	0.68	2211	17.24	0.65
4122	17.76	0.65	1207	15.46	0.40	1245	15.99	0.48	2212	11.95	1.11
4123	16.52	0.39	1208	17.20	0.58	1246	15.34	0.39	2213	15.96	0.47
4124	16.37	0.43	1209	15.63	0.41	1247	16.03	0.45	2214	15.18	0.45
4125	15.60	0.35	1210	17.21	0.62	1249	15.55	0.32	2215	15.37	0.39
4126	17.24	0.67	1211	14.76	0.36	1250	17.89	0.64	2216	16.79	0.63
4127	15.17	0.36	1212	15.05	0.42	1251	17.94	0.63	2217	14.82	0.50
4128	13.08	0.88	1214	15.35	0.39	1252	17.77	0.74	2218	15.22	0.43
4129	14.40	0.50	1215	17.68	0.70	1253	17.84	0.78	2219	17.35	0.70
4130	15.63	0.37	1216	15.74	0.48	1254	16.96	0.55	2220	15.64	0.43
4131	17.73	0.66	1217	16.06	0.89	1255	17.82	0.68	2221	17.77	0.69
4132	13.75	0.41	1218	15.37	0.41	1256	17.84	0.74	2225	17.53	0.73
4133	16.40	0.45	1219	15.06	0.40	1257	16.26	0.45	2226	17.39	0.74
4134	17.66	0.79	1220	16.13	0.44	1258	15.61	0.40	2227	17.86	0.72
4135	16.64	0.51	1221	15.75	0.43	1259	17.70	0.65	2228	16.12	0.49
4136	15.18	0.44	1222	15.52	0.37	1260	16.80	0.55	2229	17.23	0.64
4137	16.75	0.74	1223	16.26	0.45	1261	17.60	0.64	2230	18.08	0.65
4138	13.25	0.98	1224	14.85	0.46	1264	17.43	0.63	2231	17.76	0.84
4139	17.49	0.64	1225	15.10	0.42	1265	17.64	0.65	2232	16.62	0.59
4140	15.21	0.34	1226	14.91	0.41	1266	15.19	0.60	2233	16.19	0.47
4141	14.33	0.46	1227	18.06	0.70	1267	15.17	0.40	2234	16.68	0.59
4143	13.25	0.94	1228	16.24	0.46	1268	16.46	0.45	2235	16.77	0.57
4145	15.49	0.32	1229	13.07	1.01	1269	16.55	0.51	2236	17.78	0.73

TABLE 3—*Continued*

STAR	V	B-V	STAR	V	B-V	STAR	V	B-V	STAR	V	B-V
2238	17.34	1.07	2274	17.94	0.63	3228	16.53	0.50	3266	17.04	0.59
2239	16.62	0.66	2275	17.43	0.67	3229	15.60	0.91	3267	17.69	0.67
2240	17.87	0.79	2276	14.90	0.83	3230	17.75	0.69	3268	17.04	0.59
2241	15.78	0.49	2277	15.77	0.43	3231	13.12	0.99	3269	17.60	0.61
2242	16.24	0.42	2278	15.84	0.42	3232	17.13	0.65	3270	16.67	0.49
2243	17.36	0.66	2279	17.77	0.75	3233	15.79	0.42	3271	14.00	0.94
2244	17.22	0.76	2280	16.08	0.44	3235	16.37	0.56	3272	17.25	1.00
2245	17.32	0.68	2281	15.47	0.40	3236	18.06	0.66	4201	15.66	0.40
2246	16.43	0.62	2282	17.78	0.64	3239	14.96	0.39	4202	15.16	0.38
2247	15.33	0.48	2283	15.16	0.43	3240	16.01	0.42	4203	17.06	0.65
2248	17.93	0.67	2284	16.20	0.48	3241	13.82	0.13	4204	17.14	0.57
2249	14.94	0.45	2285	15.09	0.38	3242	17.54	0.75	4205	13.29	0.95
2250	16.45	0.53	2286	16.39	0.58	3243	14.69	0.84	4206	16.16	0.43
2251	13.20	0.96	3201	15.97	0.42	3244	15.60	0.38	4207	17.06	0.86
2252	15.96	0.44	3202	15.95	0.40	3245	17.93	0.65	4208	16.85	0.58
2253	16.38	0.54	3203	17.66	0.71	3246	17.99	0.60	4211	17.22	0.61
2254	12.02	0.06	3204	12.67	0.91	3247	17.06	0.67	4212	16.34	0.46
2255	13.48	0.80	3205	16.80	0.63	3248	17.32	0.56	4214	15.96	0.54
2257	14.96	0.30	3206	14.87	0.44	3249	14.69	0.36	4215	15.94	0.39
2258	15.52	0.24	3208	17.63	0.74	3250	16.72	0.50	4216	14.81	0.43
2259	15.73	0.35	3209	16.12	0.46	3251	17.53	0.70	4217	17.47	0.79
2260	16.45	0.59	3210	15.72	0.43	3252	16.07	0.54	4218	14.57	0.26
2261	17.20	0.80	3213	14.34	0.57	3253	15.81	0.44	4219	17.69	0.66
2262	14.08	0.52	3215	18.03	0.67	3254	11.08	1.38	4220	17.01	1.01
2263	17.32	0.66	3216	17.06	0.79	3255	13.06	0.81	4221	16.92	0.54
2264	16.42	0.49	3217	15.28	0.39	3256	17.40	0.65	4222	17.59	0.66
2265	14.48	0.40	3218	15.31	0.42	3257	15.80	0.45	4223	14.72	0.64
2266	15.58	0.34	3219	14.79	0.39	3258	16.33	0.52	4224	17.51	0.56
2267	17.19	0.65	3220	17.24	0.64	3259	17.52	0.77	4225	16.22	0.48
2268	15.93	0.50	3221	15.70	0.39	3260	15.02	0.53	4226	17.73	0.69
2269	14.12	0.45	3223	15.36	0.40	3261	16.79	0.61	4227	16.06	0.55
2270	15.17	0.63	3224	15.37	0.38	3262	16.13	0.85	4228	12.04	1.69
2271	15.50	0.36	3225	16.65	0.87	3263	15.08	0.37	4230	12.86	0.61
2272	16.96	0.57	3226	17.61	1.06	3264	16.23	0.45	4231	16.45	0.46
2273	12.80	0.07	3227	16.21	0.53	3265	13.21	1.05	4232	15.76	0.40

TABLE 3—*Continued*

STAR	V	B-V	STAR	V	B-V	STAR	V	B-V	STAR	V	B-V
4233	16.35	0.63	4270	17.59	0.80	1334	17.42	0.68	1378	18.03	0.33
4234	17.06	0.63	4271	17.01	0.58	1335	17.57	0.77	1379	15.16	0.37
4235	16.10	0.55	4272	15.16	0.39	1337	12.54	0.50	1380	11.88	0.54
4236	15.15	0.36	4273	16.99	0.57	1338	15.22	0.29	1381	14.80	0.31
4237	15.30	0.34	4274	13.78	0.95	1340	14.50	0.86	1382	17.07	0.53
4238	15.47	0.58	4275	16.62	0.51	1341	17.84	0.51	1383	17.27	0.63
4239	15.30	0.67	4276	16.05	0.46	1342	15.13	0.45	1384	14.92	0.43
4240	13.12	0.97	1301	14.64	0.88	1343	13.25	0.97	1385	15.80	0.42
4241	15.09	0.38	1302	15.39	0.35	1344	16.49	0.47	1386	18.09	0.74
4242	17.65	0.67	1303	17.26	0.65	1345	17.28	0.79	1387	17.85	0.81
4243	17.59	0.67	1304	16.73	0.52	1349	11.93	0.46	1389	15.54	0.39
4244	17.88	0.67	1305	14.31	0.36	1350	15.47	0.33	1390	14.69	0.41
4245	17.84	0.60	1306	15.82	0.55	1352	17.76	0.69	1391	16.28	0.62
4246	17.62	0.66	1307	16.99	0.55	1353	16.33	0.45	1392	15.47	0.89
4247	16.47	0.53	1308	15.27	0.54	1354	15.37	0.37	1393	17.18	0.61
4248	17.11	0.59	1309	16.91	0.56	1356	15.45	0.49	1394	14.82	0.42
4249	16.62	0.74	1310	16.52	0.52	1357	17.61	0.63	2301	16.10	0.41
4252	17.99	0.69	1311	15.05	0.42	1358	15.16	0.38	2302	17.68	0.67
4253	17.60	0.74	1312	17.12	0.58	1359	13.31	1.00	2303	18.08	0.67
4254	15.03	0.39	1313	15.35	0.40	1360	15.37	0.40	2305	15.62	0.38
4255	15.21	0.51	1314	16.89	0.50	1361	15.34	0.36	2306	15.39	0.38
4256	16.11	0.45	1315	16.95	0.54	1362	17.13	0.75	2308	17.19	0.67
4257	16.81	0.64	1316	15.85	0.46	1363	15.89	0.38	2309	13.07	0.99
4258	15.76	0.40	1317	17.48	0.61	1364	16.62	1.13	2311	14.68	0.49
4259	15.89	0.56	1320	13.21	0.94	1365	16.22	0.48	2312	17.71	0.74
4260	17.36	1.07	1322	18.06	0.65	1366	16.69	0.55	2313	17.79	0.67
4261	17.51	0.68	1323	17.86	0.58	1368	17.39	0.67	2314	17.24	0.69
4262	14.47	0.49	1324	15.24	0.43	1369	18.05	0.68	2315	16.33	0.60
4263	16.64	0.56	1325	13.17	0.95	1370	17.88	0.68	2316	15.81	0.43
4264	15.03	0.72	1326	16.20	0.43	1371	16.10	0.40	2317	17.62	0.66
4265	17.04	0.55	1327	16.05	0.37	1372	15.60	0.50	2318	16.82	0.56
4266	17.30	0.60	1328	14.71	0.40	1374	18.04	0.72	2319	17.60	0.69
4267	15.85	0.41	1329	16.67	0.68	1375	11.24	0.25	2320	15.90	0.43
4268	17.96	0.54	1330	15.84	0.38	1376	17.54	0.66	2321	15.53	0.37
4269	17.05	1.19	1331	14.39	0.44	1377	14.98	0.83	2322	16.33	0.56

TABLE 3—*Continued*

STAR	V	B-V	STAR	V	B-V	STAR	V	B-V	STAR	V	B-V
2323	17.54	0.72	2359	17.03	0.61	2394	15.42	0.38	3327	16.35	0.54
2324	15.17	0.37	2360	17.59	0.70	2395	15.01	0.43	3328	14.97	0.42
2325	15.51	0.39	2361	18.06	0.64	2396	17.67	0.67	3329	15.37	0.45
2326	15.76	0.44	2362	15.55	0.39	2397	16.77	0.49	3330	15.57	0.49
2327	15.65	0.41	2363	15.30	0.46	2398	17.91	0.84	3332	15.94	0.98
2328	15.06	0.40	2364	13.04	0.89	2399	17.18	0.57	3333	17.12	0.65
2329	13.15	0.96	2365	16.65	0.57	23101	13.20	0.99	3334	16.78	0.56
2330	16.46	0.52	2366	16.92	0.90	23102	16.78	0.55	3335	15.67	0.49
2331	16.30	0.44	2367	14.07	0.62	23103	14.98	0.49	3336	17.96	0.90
2332	14.95	0.43	2368	16.36	0.52	23104	15.63	0.71	3337	15.75	0.39
2333	18.08	0.68	2369	14.93	0.39	23105	15.17	0.41	3338	16.53	0.42
2334	18.02	0.44	2370	16.41	0.58	23106	15.80	0.48	3339	15.47	0.41
2335	15.80	0.51	2371	15.28	0.41	3301	17.20	0.87	3340	16.33	0.54
2336	15.42	0.65	2372	16.90	0.49	3304	17.26	1.22	3341	15.89	0.40
2338	17.12	0.63	2373	15.56	0.38	3305	14.57	0.43	3342	17.34	1.34
2339	18.08	0.65	2374	16.35	0.48	3306	17.22	0.62	3343	17.71	0.77
2340	14.90	0.37	2375	13.59	1.01	3308	15.46	0.65	3344	15.45	0.37
2341	17.93	0.70	2376	14.51	0.48	3309	18.10	0.68	3345	17.06	0.62
2342	16.95	0.71	2377	17.34	0.69	3310	17.83	0.71	3346	17.27	0.73
2343	15.42	0.40	2378	17.07	0.72	3311	17.64	0.64	3347	18.04	0.68
2344	15.80	0.43	2379	16.59	0.64	3312	15.92	0.41	3350	15.57	0.40
2345	16.17	0.46	2380	13.18	0.95	3313	14.50	0.53	3353	15.61	1.58
2346	17.88	0.63	2381	17.12	0.62	3314	17.00	0.59	3356	14.21	0.89
2347	15.00	0.44	2382	17.68	0.76	3315	16.30	0.79	3357	17.45	0.90
2348	14.72	0.49	2383	15.80	0.49	3396	15.49	0.46	3358	16.69	0.54
2349	17.27	0.78	2384	15.98	0.43	3316	10.90	1.43	3359	13.27	0.96
2350	16.79	0.70	2385	17.31	0.63	3318	15.20	0.37	3360	14.98	0.40
2351	14.00	0.58	2386	15.15	0.41	3319	17.93	0.65	3362	16.67	0.80
2352	16.48	0.55	2387	15.08	0.97	3320	17.70	0.60	3363	15.17	0.38
2353	16.46	0.55	2388	15.97	0.48	3321	15.60	0.46	3364	15.80	1.61
2354	16.14	0.45	2389	17.43	0.79	3322	16.99	0.64	3365	16.57	0.52
2355	16.30	0.60	2390	16.22	0.51	3323	15.54	0.36	3366	16.56	1.09
2356	15.60	0.38	2391	16.64	0.57	3324	13.27	0.98	3367	15.36	0.36
2357	17.11	0.62	2392	16.75	0.51	3325	16.19	0.46	3368	17.09	0.88
2358	15.95	0.43	2393	17.22	0.59	3326	16.42	0.45	3369	17.30	0.72

TABLE 3—*Continued*

STAR	V	B-V	STAR	V	B-V	STAR	V	B-V	STAR	V	B-V
3370	16.60	0.54	4313	17.18	0.58	4352	15.97	0.43			
3371	15.93	0.44	4314	17.95	0.66	4353	15.07	0.34			
3372	17.39	0.66	4315	16.60	0.47	4354	16.31	0.46			
3373	15.58	0.35	4316	17.48	0.59	4355	16.08	0.57			
3374	15.91	0.41	4317	16.18	0.54	4356	17.20	0.56			
3375	15.72	0.34	4318	15.32	0.35	4357	17.67	0.63			
3376	17.63	1.04	4320	17.70	0.68	4358	16.35	0.46			
3377	17.36	0.63	4321	18.10	0.64	4359	15.36	0.37			
3378	15.26	0.38	4322	16.74	0.49	4360	16.90	0.56			
3380	16.00	0.44	4323	17.31	0.60	4361	14.89	0.43			
3381	16.91	0.65	4325	17.26	0.62	4362	16.49	0.50			
3382	17.51	0.69	4327	17.78	0.77	4363	15.29	0.40			
3383	15.74	0.49	4328	16.46	0.53	4364	16.19	0.45			
3384	17.34	0.74	4329	17.10	0.56	4365	16.66	0.52			
3385	16.29	0.76	4330	15.91	0.47	4366	17.51	0.65			
3386	15.25	0.69	4331	15.18	0.38	4367	15.35	0.84			
3387	17.98	0.68	4332	16.76	0.68	4368	17.42	1.14			
3388	17.38	0.61	4333	15.40	0.47	4369	17.98	0.62			
3389	16.80	1.01	4334	17.00	0.58	4370	15.09	0.41			
3390	16.67	0.66	4335	16.45	0.45	4371	14.52	0.08			
3391	16.52	0.58	4337	14.71	0.42	4372	14.64	0.42			
3392	13.15	0.93	4338	14.88	0.42	4373	15.34	0.40			
3393	17.73	0.71	4339	17.43	0.70	4374	14.75	0.48			
3394	15.56	0.38	4340	16.75	0.51	4375	16.79	0.63			
3395	16.90	1.36	4341	15.93	0.44	4376	13.04	1.01			
4301	16.50	0.77	4342	17.59	0.64	4377	16.66	0.55			
4302	17.25	0.59	4343	15.96	0.88	4378	15.57	0.44			
4303	17.43	0.58	4344	16.47	1.38	4379	16.02	0.46			
4305	17.17	0.61	4345	15.65	0.57	4380	14.85	0.47			
4306	17.86	0.68	4346	16.85	0.77	4381	13.59	0.49			
4307	16.45	1.40	4347	17.25	0.54	4382	15.00	0.41			
4308	17.39	0.67	4348	17.61	0.67						
4309	15.57	0.38	4349	16.90	0.54						
4310	14.27	0.78	4350	17.59	0.75						
4312	17.73	0.71	4351	17.42	0.63						

All of the photographic photometry was done on the Cuffey iris photometer at Yale University Observatory. Color equations used in the transformation of the photographic data to the photoelectric system were similar to those used for several other clusters by the authors. These equations are: $V_{pg} = V - 0.12\,(B - V)$ for 103 aD plates, and $B_{pg} = B + 0.09\,(B - V)$ for 103 aO plates. Stars were measured within a circular area of diameter 10′ centered on the cluster, as identified on the chart shown in Figure 1 (Plate 17). The magnitudes and colors derived are listed in Table 3.

b) DDO Photometry

DDO photometry was done on 13 stars in the cluster field to aid in determining reddening and metallicity. Observational procedures followed those of McClure (1976, 1979), and the observations were done with the same equipment described above. The DDO indices are listed in Table 4 where the column labeled "*n*" again denotes the number of nights on which each star was observed.

III. THE COLOR-MAGNITUDE DIAGRAM

The color-magnitude (*C-M*) diagram constructed from all the photographic data is shown in Figure 2*a*. There are two reasons why many of the stars in this diagram scatter off the principal sequences. First, many stars are not cluster members. The galactic latitude of the cluster being only $\sim 10°$, many foreground stars are included. Second, because of its relatively large distance, the size of the cluster on the sky is small, so that crowding of images is a problem, and a few images which have been measured overlap with companions that affect the iris measurements.

Figure 2*b* and 2*c* show the *C-M* diagram for only those stars with greater than 80% and greater than 90% probability of membership on the basis of proper motions. In addition to field stars being removed from these diagrams, there are 77 of the 801 stars with iris photometry that are missing because proper motion measurements could not be made.

Examination of Figure 2 reveals that NGC 2506 is *very* similar to the other old cluster NGC 2420 (shown in Fig. 2*d* from the data of McClure, Forrester, and Gibson 1974). A number of interesting features which are common to the *C-M* diagrams of both clusters are as follows:

1. The *C-M* diagrams represent *old* clusters, and both appear to have very nearly the same age.

2. There is a "gap" in the main sequence of both clusters about 1.2 mag below the turnoff. This gap occurs at $V = 15.8$ mag in NGC 2506, and at $V = 15.3$ mag in NGC 2420. Although the significance of gaps may be questionable (e.g., there are other apparent gaps which are almost certainly spurious), their presence at the same relative positions in both cluster *C-M* diagrams appears to establish their reality. They can most likely be explained by the rapid structural change in the hydrogen exhaustion phase of stellar evolution. Another suggestion, that gaps may occur on the main sequence at the onset of convection (Bohm-Vitense and Canterna 1974) seems less likely to apply here since the cluster main sequences are too red.

3. There is a scatter of points on the red edge of the main sequence which can best be explained as due to binaries. One expects a binary sequence to lie near 0.75 mag above the main sequence in the *C-M* diagram (see § IV).

4. There is a second "gap" near the tip of the main-sequence turnoff (at $V = 14.6$ mag and $V = 14.1$ mag in NGC 2506 and NGC 2420, respectively). This "gap" was discussed in the case of NGC 2420 by McClure, Newell, and Barnes (1978) as possibly being due to the hydrogen exhaustion phase of stellar evolution, its elevation to the very tip of the turnoff being due to overshooting of the convective core. A strong disadvantage to this explanation is that one must then produce a plausible explanation for the "gap" mentioned above at $V = 15.8$ and 15.3 mag in the two-cluster *C-M* diagrams. Perhaps a better explanation for the brighter gap is that it is formed by a sequence of binary stars near 0.75 mag above the turnoff. If the binary sequence on the red side of the main

TABLE 4

DDO PHOTOMETRY

Star (1)	*P* (2)	*C*(45 − 48) (3)	*C*(42 − 45) (4)	*C*(41 − 42) (5)	*C*(38 − 41) (6)	*n* (7)	*E*(*B* − *V*) (8)	δCN (9)
1112	65	1.182	0.796	0.109	−0.566	1	0.03	−0.084
2101	0	1.162	0.780	0.060	−0.640	2	...	−0.104
2111	0	1.002	0.573	0.033	−0.807	1	...	...
2122	92	1.267	0.916	0.211	−0.459	1	0.03	−0.081
4128	...	1.165	0.724	0.123	−0.660	1	0.04:	...
4138	94	1.173	0.805	0.108	−0.565	1	0.03	−0.067
2212	95	1.223	0.878	0.161	−0.472	1	0.02	−0.079
3254	20	1.353	1.130	0.225	−0.229	2	0.09	−0.119
3255	71	1.071	0.720	0.058	−0.634	1	...	...
4228	0	1.446	1.319	0.218	−0.030	1	0.13	−0.100
1375	0	0.824	0.383	0.056	−0.895	2	...	...
3316	30	1.318	1.143	0.264	−0.161	1	...	−0.040
2401	...	1.420	1.327	0.241	−0.001	1	0.05	−0.055

PLATE 17

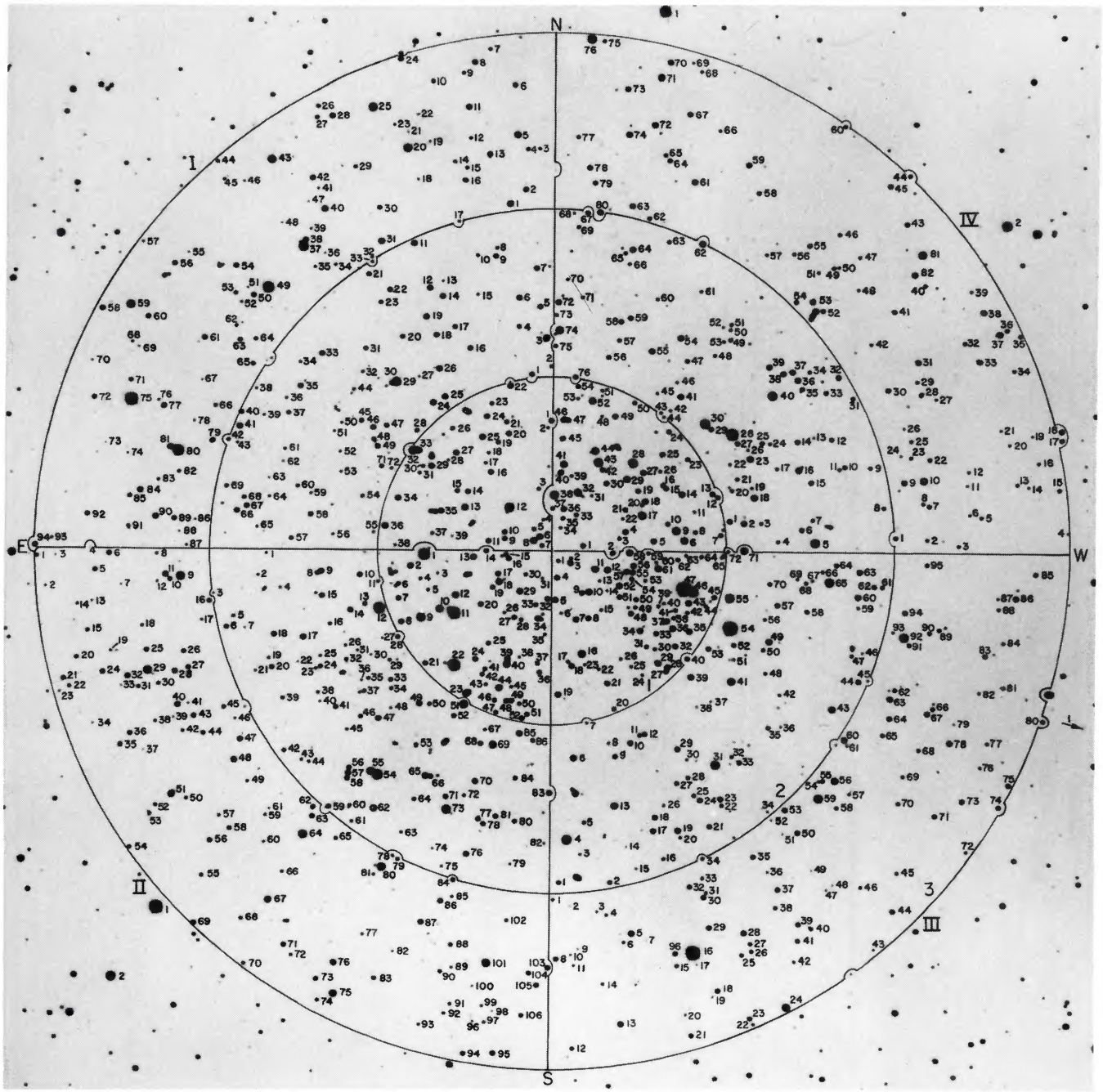

FIG. 1.—Identification chart for stars in NGC 2506 from a 45 min V exposure with the CTIO 1.5 m telescope. In all tables, the first digit of star numbers represents the sector and the second digit the ring number from this chart.

McCLURE, TWAROG, AND FORRESTER (*see* page 849)

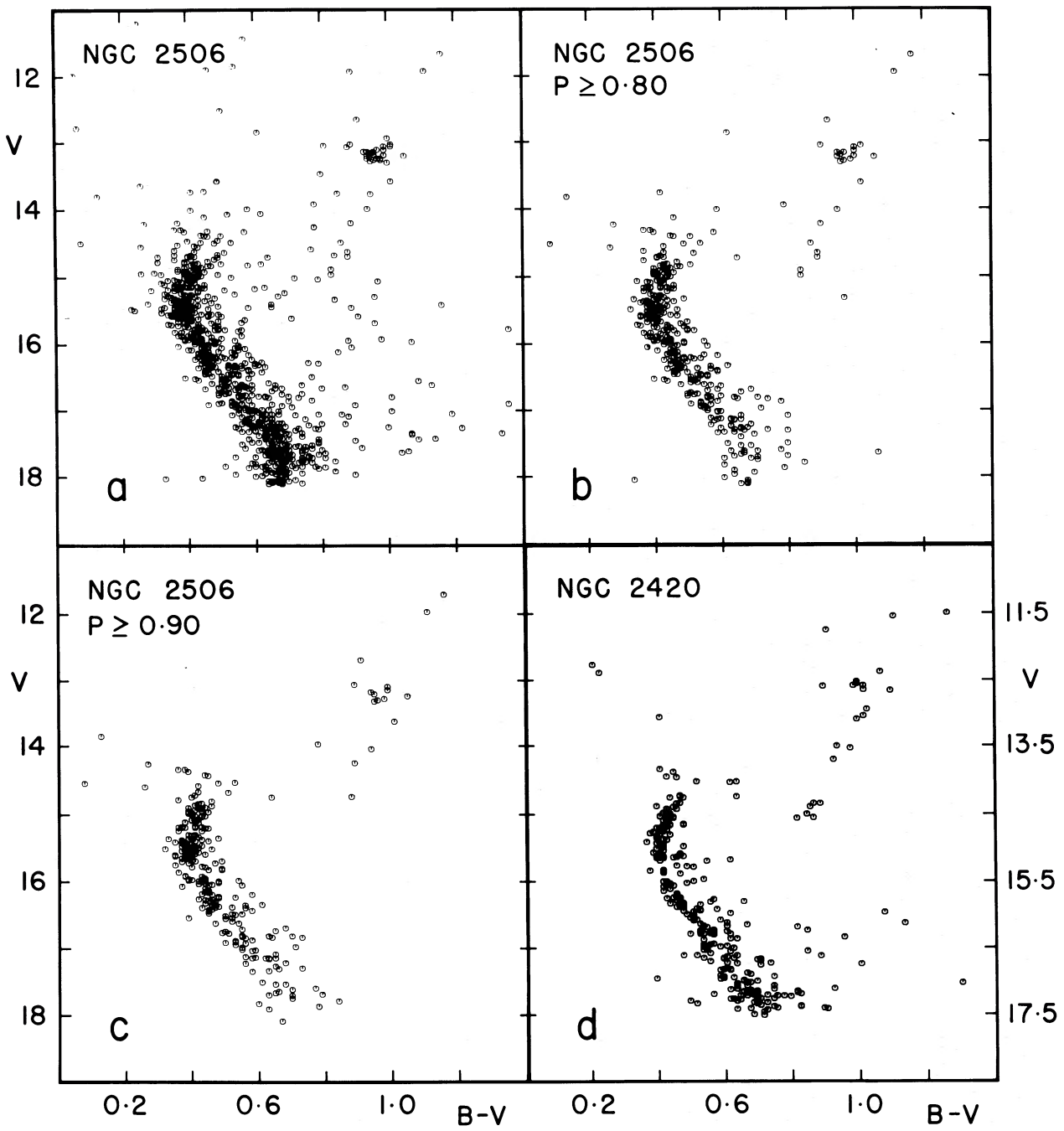

FIG. 2.—The *C-M* diagram for NGC 2506 for (a) all stars, (b) stars with membership probabilities >80%, (c) stars with membership probabilities >90%. For comparison, the *C-M* diagram of NGC 2420 is shown in (d). These data are taken from McClure *et al.* (1974) and include only proper motion members for stars brighter than $V = 15.8$ mag.

sequence is real (see § IV), then one should also expect to find binaries above the tip of the turnoff.

5. There appear to be numerous bright blue stragglers in both clusters which are proper motion members (see discussion by Chiu and van Altena 1981). Such stars also exist in the old cluster M67 (Murray, Corben, and Allchorn 1965) and Melotte 66 (Anthony-Twarog, Twarog, and McClure 1979).

6. The giant-branch "clump," about 1.5 mag above the main-sequence turnoff, is very prominent in both *C-M* diagrams as it is for other old clusters (see Cannon 1970). The only other old cluster *C-M* diagram in which no such clump is obvious is that of NGC 188 (see Anthony-Twarog *et al.* for discussion).

7. There are giant stars which appear to be brighter than the normal giant branch in both clusters, although there are only two such stars in NGC 2506 that are proper motion members. Such stars have also been discussed by Hawarden (1976*b*, 1978) and Anthony-Twarog, Twarog, and McClure (1979) in the case of the old cluster Melotte 66. The most plausible explanation for these stars seems to be that they are asymptotic giant-branch stars, in a post–horizontal-branch phase of evolution.

IV. FREQUENCY OF BINARIES

An important question from the standpoint of both stellar evolution and the dynamical evolution of clusters is what percentage of stars that we see on or away from the main sequence are binaries. While the only definitive ways of locating binaries are those based on spectroscopic detection, or variability, attempts have been made to estimate the frequency of binaries by recognizing that the addition of a secondary star produces a deviation from the ZAMS which is detectable if the effect is significantly larger than the photometric uncertainty of the data. Unfortunately, the interpretation of such analyses is uncertain because (1) estimates of the mass-ratio distribution and the percentage of binaries are strongly dependent on where one locates the ZAMS (Bettis 1975; Jaschek 1976; Dabrowski and Beardsley 1977; Trimble and Ostriker 1978), and (2) deviations from the main sequence can occur for reasons other than the presence of binaries, e.g., rotation. In the case of NGC 2506, however, the latter effect is unlikely to be important since the main sequence includes only late-type stars which are unlikely to be fast rotators.

If binaries are the cause of scatter above the ZAMS in NGC 2506, the deviation from the ZAMS should be determined by $q(\alpha)$, the mass-ratio distribution of binaries. The work of Trimble (1978) has demonstrated that the best data for field stars lead to a bimodal distribution for $q(\alpha)$ with peaks at α (i.e., M_1/M_2) of 0.3 and 1.0 and a minimum at 0.7. If we assume that the $q(\alpha)$ for cluster stars is the same as for the field, it is possible to predict what the deviation from the ZAMS should look like. We should expect that at any given color, as one moves away from the ZAMS, the distribution will first show a large dispersion caused by the combined effects of the photometric errors and the dispersion of the first peak of the $q(\alpha)$ distribution of binaries. There should then be a minimum approximately 0.4–0.6 mag above the ZAMS followed by a second peak 0.6–0.9 mag above the ZAMS, created by the secondary peak in $q(\alpha)$. As noted by Dabrowski and Beardsley (1977), it is possible to find binaries more than 0.75 mag above the ZAMS because of the combined effects of the integrated magnitudes and the shift to redder colors.

To test this effect in NGC 2506 we have divided the main sequence between $B - V$ of 0.44 and 0.68 mag into bins 0.04 mag wide. The distribution in each bin for all stars with membership greater than 90% can be seen in Figure 3. While the location of the primary peak in the distribution is uncertain, the overall shape of the distribution is exactly what one expects if the deviations are caused by binaries. By making use of the field star function for $q(\alpha)$, which may or may not apply to clusters (see Abt 1979), we make a very crude estimate that half the stars in NGC 2506 are binaries.

V. REDDENING AND METAL ABUNDANCE

Column (8) of Table 4 lists values of reddening based on DDO and $B - V$ photometry of giants using the calibration of Janes (1977). For the four giants that have greater than 50% membership probability, the mean value of reddening is $E(B - V) = 0.03$ mag, with a very small dispersion. For all stars regardless of membership, the mean reddening is $E(B - V) = 0.05 \pm 0.01$ mag. Since there is no reason to believe that field stars in the direction of this high-latitude cluster should exhibit reddening values that are too high, the latter value based on the larger number of stars will be adopted. This value is also consistent with that deduced below on the basis of the *UBV* color-color diagram.

Figure 4 shows the color-color diagram for members that have photoelectric *UBV* photometry. The colors have been corrected for a reddening of $E(B - V) = 0.05$ mag and the corresponding $E(U - B)$ based on the slope of the reddening line shown as a function of $B - V$ in Figure 7 of Crawford and Mandwewala (1976). The solid curves represent the intrinsic sequences for Hyades dwarfs (Sandage and Eggen 1959) and Hyades moving group giants (Eggen 1966*b*). The dashed curves represent intrinsic sequences for turnoff stars 1 mag and 2 mag above the ZAMS, taken from Eggen (1966*a*) and Eggen and Sandage (1964).

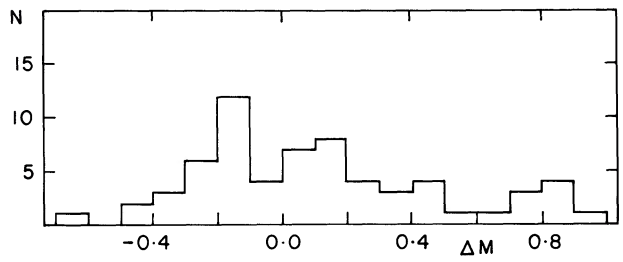

FIG. 3.—The distribution of stars across the main sequence in NGC 2506 for those stars with membership probabilities > 90%.

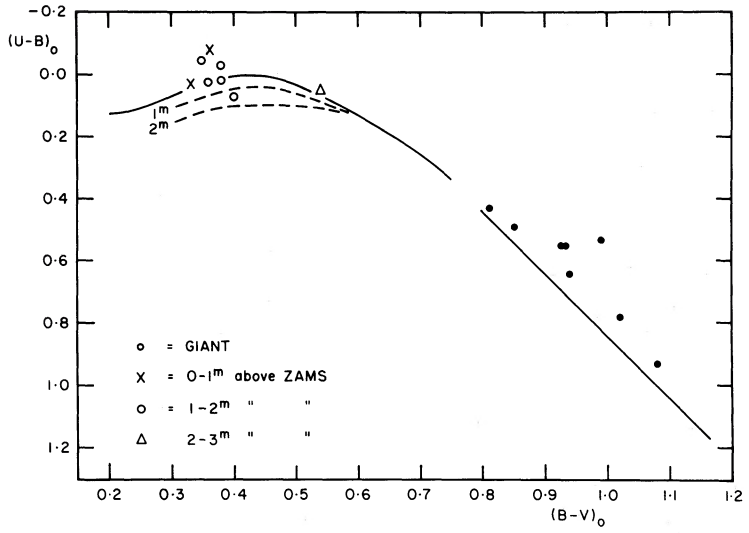

FIG. 4.—The color-color diagram for members with photoelectric *UBV* photometry. Corrections for reddening corresponding to $E(B-V) = 0.05$ mag have been applied. The curves represent the Hyades main sequence and Hyades moving group giant sequence. The dashed curves represent sequences for evolved turnoff stars 1 mag and 2 mag above the ZAMS.

Column (7) of Table 1 lists ultraviolet excesses for cluster members based on the positions of stars in this diagram relative to the appropriate sequences, and with the correction suggested by Sandage (1969) for the guillotine effect applied to the main-sequence turnoff stars. A mean ultraviolet excess of $\delta(U-B) = 0.09$ mag is derived from both giants and turnoff stars, ignoring star 3265 which has a discrepant value more than two standard deviations from the mean. If $E(B-V)$ is changed by several hundredths of a magnitude, the $\delta(U-B)$ values for turnoff stars and giants change in opposite directions, but the *mean* value for all stars remains the same, and $\delta(U-B) = 0.09 \pm 0.01$ mag appears well established. By consulting the calibrations of Wallerstein (1962), Eggen (1964), Wallerstein and Helfer (1966), and Branch and Alexander (1973), we derive a metal abundance relative to the Hyades of [Fe/H] = −0.55.

A measurement of ultraviolet excess can also be obtained from the $[C_0(38-42), C_0(45-48)]$-plane of the DDO systems (Fig. 5), as Norris and Hawarden (1978) have discussed in the case of the old disk cluster NGC 2243. In Figure 5 the solid curves are Population I intrinsic sequences. Proper motion members of NGC 2506 are represented by large filled circles, nonmembers by open circles, and other stars with nonzero membership probability or with no membership data by

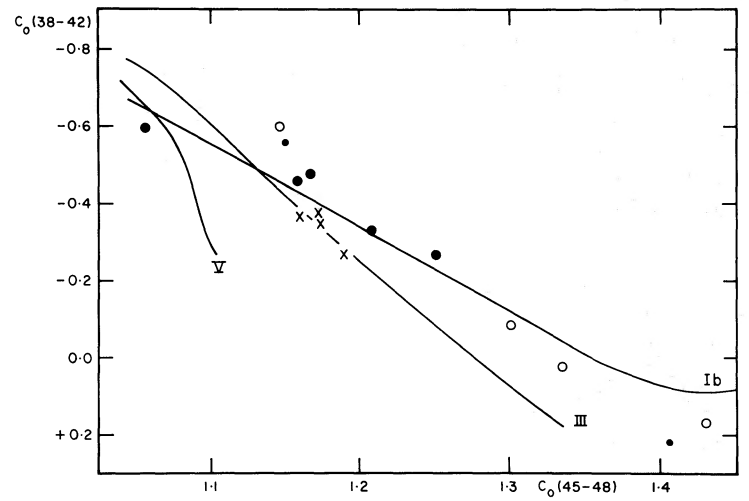

FIG. 5.—The DDO ultraviolet excess diagram for giant stars in NGC 2506. The curves represent Population 1 solar neighborhood stars. Large filled circles represent proper motion members, open circles nonmembers, and small filled circles other stars with nonzero membership probability or no proper motion data. Crosses represent Hyades giants. Lowering metal abundance shifts stars upward in this diagram.

small filled circles. The values for the four Hyades giants are also plotted on the diagram as crosses.

Unfortunately, the errors are large because of the limited amount of DDO photometry that was done, but it is obvious that NGC 2506 is metal poor relative to the Hyades and other solar neighborhood giants. Since the cluster NGC 2506 is a member of the disk population, it is perhaps better to compare the NGC 2506 stars with the Hyades giants rather than with 47 Tucanae giants as Norris and Hawarden did in the case of NGC 2243. The scatter for 47 Tucanae values in this plane is quite large, due possibly to a spread in CN strengths (see Hartwick and McClure 1980) which exists for stars in the globular cluster. A mean ultraviolet excess $\delta 3842 = 0.12 \pm 0.03$ mag is obtained for the four NGC 2506 members closest to the Hyades in temperature. Adopting Osborn's (1971) relation of $[Fe/H] = -5.7\ \delta 3842$, we derive $[Fe/H] = -0.7 \pm 0.2$ relative to the Hyades.

Column (9) of Table 3 lists values of the DDO cyanogen anomaly δCN derived using the method of Janes (1975). The mean value for cluster members is -0.08 ± 0.01 mag. This implies a heavy element abundance of $[Fe/H] = -0.7$ relative to the Hyades if the calibration of CN versus iron abundance given by Janes (1975) is adopted.

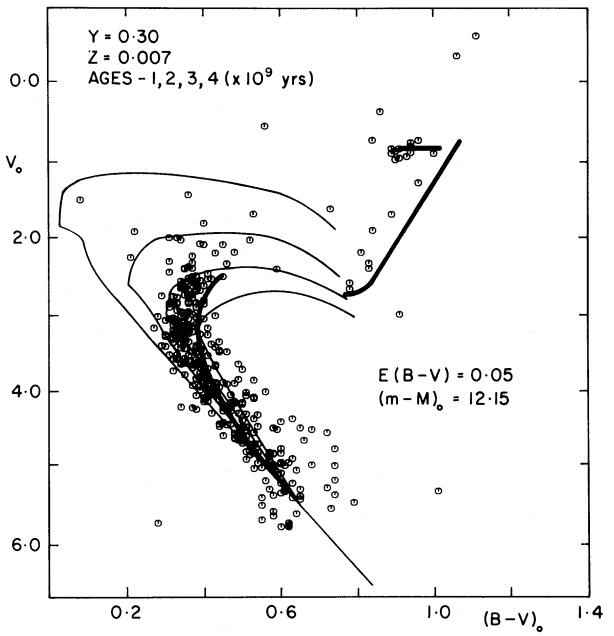

FIG. 6.—The *C-M* diagram for NGC 2506 stars with membership probability > 80%. The heavy curve is a schematic representation of the *C-M* diagram for NGC 2420. Both clusters are fitted to isochrones for heavy element abundance $Z = 0.007$ and helium abundance $Y = 0.30$ taken from the Yale models as described in the text.

VI. COMPARISON OF NGC 2506 AND NGC 2420

NGC 2506 is very close to the old cluster NGC 2420 in metal abundance. The mean ultraviolet excess $\delta(U - B) = 0.09 \pm 0.01$ mag compares with $\delta(U - B) = 0.01 \pm 0.01$ mag for NGC 2420 from the data of McClure, Forrester, and Gibson (1974). The cyanogen anomaly for NGC 2506 of δCN $= -0.08 \pm 0.01$ mag compares with δCN $= -0.06 \pm 0.01$ mag for NGC 2420.

Figure 6 shows the $C - M$ diagram of NGC 2506 with a schematic diagram for NGC 2420 (*heavy curves*) superposed. Both sets of data have been corrected for reddening appropriate to the cluster and fitted to isochrones for heavy element abundance $Z = 0.007$ and helium abundance 0.30. These isochrones which were published by Ciardullo and Demarque (1977) are based on a grid of evolutionary tracks computed by Mengel *et al.* (1979). The conversion to the observational plane was made by Ciardullo and Demarque (1979) using model atmosphere data. The Hyades main sequence fits a similar set of isochrones for helium abundance $Y = 0.30$ and distance modulus 3.30, approximately that suggested by van Altena (1974), Hanson (1975, 1979), and Anthony-Twarog and Demarque (1977).

Although NGC 2506 is very similar to NGC 2420, as discussed in § III, there are several differences which we can point out from Figure 6. First, NGC 2506 is slightly younger than NGC 2420, as seen from its bluer and brighter turnoff. Ages of $3.4 \pm 0.2 \times 10^9$ years and $3.8 \pm 0.2 \times 10^9$ years respectively are derived. For comparison, ages of 3.2 and 5.0×10^9 years are derived for M67 and NGC 188 respectively when fitted to similar isochrones for the appropriate metal abundance.

A second difference is the color of the giant branch. The NGC 2506 giant branch and clump is significantly bluer than that of NGC 2420, even though it is not more metal poor on the basis of its ultraviolet excess. The difference in age between the two clusters can account for some of this difference in the giant branches, but quantitatively the amount is barely significant. It is possible that the slightly weaker CN index for NGC 2506, even though its ultraviolet excess is slightly less than that of NGC 2420, represents a real difference in nitrogen/iron abundance. This can affect the relative positions of the giant and main sequences as discussed by Demarque and McClure (1977) and produce the difference in giant-branch color shown by Figure 6.

If the luminosity function of the two clusters is compared, it is clear that the giant branch of NGC 2506 is sparse relative to that of NGC 2420. Relative to main-sequence stars, NGC 2420 has 2.3 times the number of giant branch (nonclump) stars, but an equal number of clump stars. In particular, NGC 2420 has numerous low-luminosity subgiants, whereas NGC 2506 has a pronounced Hertzsprung gap. These differences in luminosity function support the contention from main-sequence fitting that there is a small difference in age between the two clusters.

VII. DISCUSSION

We have shown that NGC 2506 is very similar in age and metal abundance to NGC 2420, both clusters being located several kpc beyond the solar orbit in the direction

of the galactic anticenter. Recent work of Hawarden (1975, 1976*a*, *b*), van den Bergh (1977), Dawson (1978), Norris and Hawarden (1978), Anthony-Twarog *et al.*, and Janes (1979) on NGC 2158, NGC 2204, NGC 2243, and Melotte 66, as well as the present study of NGC 2506 has demonstrated the existence of a whole class of well-studied clusters, for which NGC 2420 is the prototype, that are old ($3–7 \times 10^9$ years), moderately metal-poor ($-0.4 > [Fe/H] > -0.7$), and situated at galactocentric distances significantly larger than the Sun's orbit. The well-known clusters NGC 188 and M67 are of comparable age to these clusters and situated at comparable distances above the galactic plane. However, they are at approximately the solar distance from the galactic center and have approximately solar metal abundance. These facts imply that the NGC 2420 class of clusters have low metal abundance due to a radial gradient of metal abundance of clusters in the galactic plane as suggested by Arp (1962) and Janes (1979).

We wish to thank Robin Ciardullo and Dr. Pierre Demarque for providing isochrone data in advance of publication, and Drs. George Chiu and Bill van Altena for undertaking the proper motion measurements on which this paper so heavily relies. This work was supported by the National Science Foundation through grant No. AST 77-25680.

REFERENCES

Abt, H. A. 1979, *A.J.*, **84**, 1591.
Anthony-Twarog, B. J., and Demarque, P. 1977, *Astr. Ap.*, **57**, 471.
Anthony-Twarog, B. J., Twarog, B. A., and McClure, R. D. 1979, *Ap. J.*, **233**, 188.
Arp, H. 1962, *Ap. J.*, **136**, 66.
Bettis, C. L. 1975, *Pub. A.S.P.*, **87**, 707.
Bohm-Vitense, E., and Canterna, R. 1974, *Ap. J.*, **194**, 629.
Branch, D., and Alexander, J. B. 1973, *M.N.R.A.S.*, **161**, 409.
Cannon, R. D. 1970, *M.N.R.A.S.*, **150**, 111.
Chiu, L.-T. G., and van Altena, W. F. 1981, *Ap. J.*, in press.
Ciardullo, R. D., and Demarque, P. 1977, *Trans. Yale Univ. Obs.*, **33**, 1.
———. 1979, in *Problems of Calibration of Multicolor Photometric Systems*, Dudley Obs. Report, No. 14, p. 317.
Cousins, A. W. J. 1973, *Mem. R.A.S.*, **77**, 223.
Crawford, D. L., and Mandwewala, N. 1976, *Pub. A.S.P.*, **88**, 917.
Dabrowski, J. P., and Beardsley, W. R. 1977, *Pub. A.S.P.*, **89**, 225.
Dawson, D. W. 1978, *A. J.*, **83**, 1424.
Demarque, P., and McClure, R. D. 1977, *Ap. J.*, **213**, 716.
Eggen, O. J. 1964, *A.J.*, **83**, 1424.
———. 1966*a*, *Roy. Obs. Bull.*, No. 120.
———. 1966*b*, *Roy. Obs. Bull.*, No. 125.
Eggen, O. J., and Sandage, A. R. 1964, *Ap. J.*, **140**, 130.
Hanson, R. B. 1975, *A.J.*, **80**, 379.
———. 1979, in *IAU Symposium No. 85, Star Clusters*, ed. J. E. Hesser and K. C. Freeman (Dordrecht: Reidel), p. 71.
Hartwick, F. D. A., and McClure, R. D. 1980, *Ap. J.*, **235**, 470.
Hawarden, T. G. 1975, *M.N.R.A.S.*, **173**, 801.
———. 1976*a*, *M.N.R.A.S.*, **174**, 225.
———. 1976*b*, *M.N.R.A.S.*, **174**, 471.
———. 1978, *M.N.R.A.S.*, **182**, 31P.
Janes, K. A. 1975, *Ap. J. Suppl.* **29**, 161.
———. 1977, *Pub. A.S.P.*, **89**, 576.
———. 1979, *Ap. J. Suppl.*, **39**, 135.
Jaschek, C. 1976, *Astr. Ap.*, **50**, 185.
King, I. R. 1964, *Roy. Obs. Bull.*, No. 82.
Landolt, A. U. 1973, *A.J.*, **78**, 959.
McClure, R. D. 1976, *A.J.*, **81**, 182.
———. 1979, in *Problems of Calibration of Multicolor Photometric Systems*, Dudley Obs. Report No. 14, p. 83.
McClure, R. D., Forrester, W. T., and Gibson, J. 1974, *Ap. J.*, **189**, 409.
McClure, R. D., Newell, B., and Barnes, J. V. 1978, *Pub. A.S.P.*, **90**, 170.
Mengel, J. G., Sweigart, A. V., Demarque, P., and Gross, P. G. 1979, *Ap. J. Suppl.*, **40**, 733.
Murray, C. A., Corben, P. M., and Allchorn, M. A. 1965, *Roy. Obs. Bull.* No. 91.
Norris, J., and Hawarden, T. G. 1978, *Ap. J.*, **223**, 483.
Osborn, W. 1971, *Ph.D. thesis*, Yale University.
Purgathofer, A. 1964, *Zs. Ap.*, **59**, 79.
Sandage, A. 1969, *Ap. J.*, **158**, 1115.
Sandage, A., and Eggen, O. J. 1959, *M.N.R.A.S.*, **119**, 278.
Trimble, V. L. 1978, *Observatory*, **98**, 163.
Trimble, V. L., and Ostriker, J. P. 1978, *Astr. Ap.*, **63**, 433.
van Altena, W. F. 1974, *Pub. A.S.P.*, **86**, 217.
van den Bergh, S. 1977, *Ap. J.*, **215**, 89.
Wallerstein, G. 1962, *Ap. J. Suppl.*, **6**, 407.
Wallerstein, G., and Helfer, H. L. 1966, *A.J.*, **71**, 350.

W. T. Forrester: Space Sciences Institute, 3625 E. Ajo Way, Tucson, AZ 85713

R. D. McClure: Dominion Astrophysical Observatory, 5071 W. Saanich Road, Victoria, B.C., V8X 4M6

B. A. Twarog: Yale University Observatory, Box 2023, Yale Station, New Haven, CT 06520